



Pergamon

Materials Research Bulletin, Vol. 33, No. 4, pp. 655–661, 1998
Copyright © 1998 Elsevier Science Ltd
Printed in the USA. All rights reserved
0025-5408/98 \$19.00 + .00

PII S0025-5408(98)00005-1

SYNTHESIS, PROPERTIES, SINTERING AND MICROSTRUCTURE OF SPHENE, CaTiSiO_5 : A COMPARATIVE STUDY OF COPRECIPITATION, SOL-GEL AND COMBUSTION PROCESSES

M. Muthuraman and K.C. Patil*

Department of Inorganic and Physical Chemistry, Indian Institute of Science,
Bangalore 560 012, India

(Refereed)

(Received May 26, 1997; Accepted June 5, 1997)

ABSTRACT

Sphene (CaTiSiO_5), a titanosilicate ceramic considered as a host material for the immobilization of radioactive waste from nuclear power reactors, has been prepared using coprecipitation, sol-gel, and solution combustion methods. All these processes initially yielded amorphous powders, which on further calcination, crystallized to yield sphene along with perovskite, titania, and cristobalite. The coprecipitation-derived powder calcined at 1000°C for 2 h showed the formation of single phase sphene; whereas, the sol-gel-derived and combustion-derived powders required higher temperature (1200°C for 2 h) for single phase sphene to form. Coprecipitation-derived sphene powder achieved 96% theoretical density when sintered at 1300°C for 2 h, and the microstructure of the sintered body showed a uniform grain size of $\approx 1 \mu\text{m}$. © 1998 Elsevier Science Ltd

KEYWORDS: A. oxide, B. chemical synthesis, D. microstructure

INTRODUCTION

Sphene (CaTiSiO_5) is the major crystalline phase in titanosilicate glass-ceramics and is being considered as a candidate for the immobilization of radioactive waste produced in nuclear power reactors [1]. Sphene crystals are thermodynamically stable in granitic groundwater and can incorporate many of the waste fission products and actinides, forming a solid solution [2].

*To whom correspondence should be addressed.

In the continuation of our studies on the synthesis of oxide materials for radioactive waste immobilization by the combustion method [3–5], we now report the synthesis of sphene by coprecipitation, sol-gel, and combustion methods. The effect of preparative techniques on the powder characteristics, crystallization sequence, sintering, and microstructure of sphene are of interest. Surface area and particle size measurements, thermogravimetric and differential thermal analysis (TG-DTA), powder X-ray diffraction (XRD), and scanning electron microscopy have been employed in this investigation.

EXPERIMENTAL

Sample Preparation. Sphene (CaTiSiO_5) was prepared by three different routes: coprecipitation (sphene-I), sol-gel synthesis (sphene-II), and solution combustion (sphene-III).

Coprecipitation. In the coprecipitation route, an aqueous solution containing calcium nitrate, titanyl chloride, and hexafluorosilicic acid was precipitated as hydroxide, using ammonium hydroxide. Titanyl chloride (TiOCl_2) was prepared by diluting TiCl_4 in HCl under an ice-cold condition. Hexafluorosilicic acid was prepared by dissolving fumed silica in a minimum amount of 5% aqueous HF. This reaction can be reversed to get hydroxide of silicon in an alkaline medium in which the alkalinity is in excess of what is required for the neutralization of hexafluorosilicic acid [6].

In the actual synthesis, an aqueous solution containing equimolar amounts of calcium nitrate, titanyl chloride, and hexafluorosilicic acid (0.2 M of each element) was precipitated by the slow addition of dilute NH_4OH . The precipitate was washed with distilled water to remove the excess ammonium hydroxide and dried in an air oven at 100°C for 12 h. The dried hydroxide powder (sphene-I) was precalcined at 700°C for 2 h to remove adsorbed water and hydroxides and further calcined at higher temperatures to study the thermal phase evolution.

Sol-Gel Synthesis. Calcium nitrate, tetraethyl orthosilicate (TEOS), $\text{Si}(\text{OC}_2\text{H}_5)_4$, and *n*-butyl titanate, $\text{Ti}(\text{O}i\text{Bu})_4$ were used in the sol-gel synthesis of sphene. An ethanolic solution of (TEOS) was mixed with an ethanolic solution of $\text{Ti}(\text{O}i\text{Bu})_4$ in a stoichiometric amount and the clear solution was stirred well for 1/2 h. HNO_3 (0.2 M) per mol of *n*-butyl titanate was added before mixing with TEOS to avoid the formation of cloudy titanium-rich precipitate and to keep the ethanolic solution of *n*-butyl titanate clear [7]. The alkoxide/alcohol molar ratio was maintained at approximately 1:100. Hydrolysis of this alkoxide mixture was carried out by adding an aqueous solution of calcium nitrate in sphene stoichiometry, and the alkoxide/water molar ratio was maintained at 1:20. The clear solution thus obtained was stirred for 1 h and then allowed to gel over a water bath. The gel formed was dried in an air oven at 100°C for 12 h. The dried gel (sphene-II) was precalcined at 700°C for 2 h to remove the organics and nitrates.

Solution Combustion. Sphene-III was prepared by the combustion of an aqueous redox mixture comprising stoichiometric amounts of calcium nitrate, titanyl nitrate, fumed silica, and carbonylhydrazide ($\text{H}_3\text{N}_2\text{CON}_2\text{H}_3$). Titanyl nitrate was prepared from titanium tetrachloride as reported earlier [5]. Fumed silica (surface area $\approx 200 \text{ m}^2/\text{g}$) was used as the source of silicon and was dispersed in the redox mixture. The stoichiometry of the redox mixture was calculated as described elsewhere [3]. The combustion reactions were carried out in a muffle furnace preheated at 450°C . The heterogeneous redox mixture undergoes rapid dehydration to form a gel-like mass,

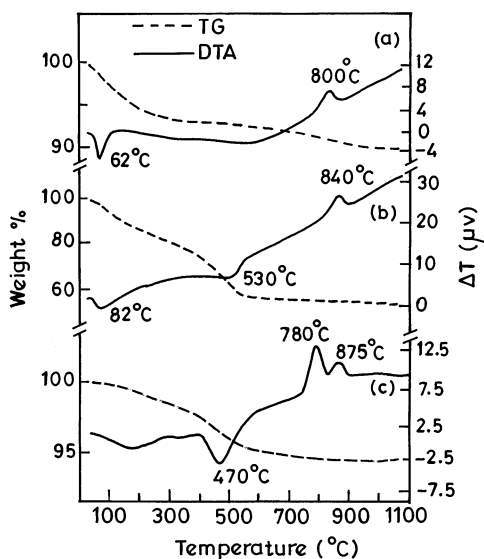


FIG. 1

TG-DTA of (a) sphene-I, (b) sphene-II, and (c) sphene-III.

which froths, foams, and ignites to burn to yield a white foamy mass. The actual composition of the heterogeneous redox mixture used for combustion synthesis was 6 g of calcium nitrate, 4.77 g of titanyl nitrate, 1.29 g of fumed silica, and 5.72 g of carbohydrazide.

Product Analysis. Simultaneous TG-DTA (Polymer Laboratories, model STA 1500) of the sphene powders (sphene-I, -II, and -III) was performed. Room temperature powder XRD patterns recorded on an Shimadzu XD-D1 X-ray diffractometer (with Ni-filtered Cu $K\alpha$ radiation) was used to identify the various phases. Samples were calcined in alumina boats at various temperatures in air with a soaking period of 2 h to study the sphene phase evolution. The powder properties were evaluated by BET surface area measurement (Micrometrics Instrument Corp., model 2100E Accusorb, Norcross, GA), particle size analysis (Seishin, model SKC 2000 micron photosizer), and density measurements. Sintering of compacted powders was carried out at 1200–1325°C in air at a heating rate of 10°C/min and a soaking period of 2 h. The sintered pellets were polished and etched with 5% HF for 20 s for the microstructure investigation using a scanning electron microscope (Jeol, model JSM-840 A).

RESULTS AND DISCUSSION

Thermal Phase Evolution. The simultaneous TG-DTA for sphene-I showed a weight loss of about 7% in the temperature range 60–300°C and an endotherm around 60°C (Fig. 1a). This could be attributed to the removal of adsorbed moisture and ammonia. Sphene crystallization occurred at 800°C, as observed by an exotherm.

TG-DTA of sphene-II is shown in Figure 1(b). The initial weight loss of about 8% in the temperature range 60–140°C and the corresponding endothermic peak results from the evaporation of alcohol and adsorbed moisture. The second-step weight loss in the temperature range of 350–550°C can be attributed to the pyrolysis of organic compounds such as

TABLE 1
Thermal Phase Evolution in Sphene-I, Sphene-II, and Sphene-III Powders

Sphene	Calcination temperature (°C)	Phase (from XRD)
I	as-dried (100)	amorphous
	700	a-TiO ₂ + SiO ^a
	850	CaTiSiO ₅ + a-TiO ₂ + SiO ^a
	1000	CaTiSiO ₅
II	as-dried (100)	amorphous
	700	a-TiO ₂ + CaTiO ₃
	900	CaTiSiO ₅ + a-TiO ₃ + CaTiO ₂
	1200	CaTiSiO ₅ + trace of CaTiO ₃ and cristobalite SiO ₂
III	as-prepared	amorphous + CaO + r-TiO ₂
	600	CaTiO ₃ + CaO + r-TiO ₂
	800	CaTiSiO ₅ + CaTiO ₃ + r-TiO ₂
	875	CaTiSiO ₅ + CaTiO ₃ + cristobalite SiO ₂
	1200	CaTiSiO ₅

^aSiO: JCPDS card 30-1127.

ethyl and isobutyl alcohols or species formed during the hydrolysis reaction and the gelation process. The total weight loss observed was 45%. The exotherm at 840°C may be due to the crystallization of sphene. Sphene-III shows a weight loss of approximately 5% around 500°C, and there is no weight loss above this temperature (Fig. 1c). DTA trace shows one endothermic peak at 470°C and two exothermic peaks at 780°C and 875°C. The endotherm may be due to the removal of impurities such as trapped nitrate ions and adsorbed water, as confirmed by the IR studies reported earlier [3].

The sphene-I and sphene-II powders were amorphous to X-ray, whereas sphene-III showed weak reflections corresponding to CaO and rutile titania (r-TiO₂). The various phases formed during calcination of the sphene precursor powders are summarized in Table 1. Precalcination of sphene-I at 700°C showed strong XRD reflections at 'd' values 3.153, 1.928, and 1.650, which could be assigned to SiO phase (JCPDS card no. 30-1127), and this phase was observed up to 800°C. Sphene phase began to appear above 800°C, and single phase sphene was formed at 1000°C (Fig. 2a).

The precalcined (700°C) sphene-II powder showed reflections corresponding to anatase titania (a-TiO₂) and CaTiO₃. Around 900°C, sphene phase began to appear at the expense of a-TiO₂ and CaTiO₃. Even after calcination at 1200°C, traces of CaTiO₃ and cristobalite SiO₂ were observed in the XRD pattern, which may be due to the homocondensation of some Si and Ti alkoxides [8]. CaTiO₃ and cristobalite SiO₂ impurities disappeared above 1200°C.

The XRD pattern of sphene-III calcined at 600°C shows calcium titanate as the major phase along with CaO and r-TiO₂. On further calcination at higher temperatures, CaTiO₃, CaO, and r-TiO₂ appeared to react with SiO₂, which is probably present in the amorphous state, to form CaTiSiO₅. The exothermic peak at 780°C in DTA could be assigned to the crystallization of sphene, confirmed by the appearance of XRD peaks corresponding to sphene on calcination at 800°C. α-Cristobalite emerged as a secondary intermediate phase between 850 and 1000°C, as reported in the literature [9]. The exothermic peak at 875°C may be due to cristobalite SiO₂, which appeared as a secondary intermediate phase in the

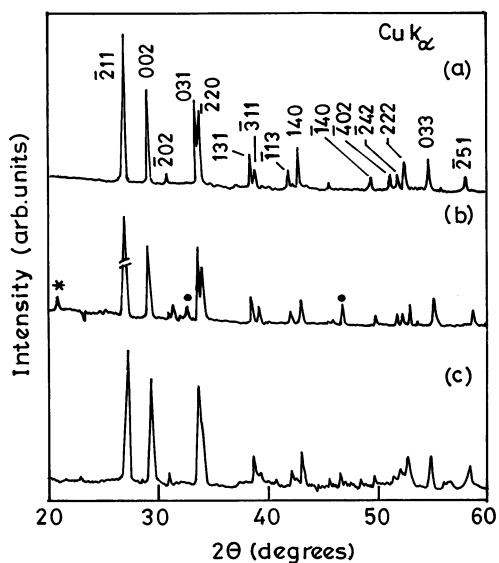


FIG. 2

Powder XRD patterns: (a) sphene-I, 1000°C; (b) sphene-II, 1200°C; and (c) sphene-III, 1200°C (* SiO_2 , ● CaTiO_3).

temperature range 875–1000°C. As the formation of CaTiSiO_5 progressed, the amount of CaTiO_3 and SiO_2 decreased, and a single phase sphene was formed after calcination at 1200°C. The sphene crystallization temperature was $\approx 50^\circ\text{C}$ lower than that of sol-gel-derived sphene (830°C) reported in the literature [10].

The sphene crystallization temperature for sphene-III was 20–60°C, lower than that for sphene-I and sphene-II. However, the sphene-I powder crystallized at a faster rate above 900°C, and single phase sphene was formed at 1000°C, which is about 200°C lower than the temperature required for sphene-II and sphene-III powders. This could be attributed to the mineralizing effect of some adsorbed fluoride ions, which favors the formation of sphene phase at lower temperature in sphene-I. A similar mineralizing effect has been observed in the preparation of zircon (ZrSiO_4)-based pigments [11], where NaF is deliberately added as a mineralizer to reduce the zircon formation temperature.

Particulate Properties. The particulate properties of various sphene powders are summarized in Table 2. The sphene-III powder is highly agglomerated, compared to sphene-I and sphene-II powders. In the case of sphene-I and sphene-II, the particle size measurements were done after precalcination at 700°C. In sphene-III, most of the particles have an agglomerated particle size of $\approx 10\ \mu\text{m}$, and the 50% average agglomerated particle size is 9.0 μm . The larger agglomerated particle size of the combustion-derived powder may be due to the higher flame temperature ($\approx 1100^\circ\text{C}$) observed during combustion. Also, the dispersed silica fume tends to aggregate when the volume of the aqueous heterogeneous redox mixture is reduced during combustion reaction. The 50% average agglomerated particle sizes of sphene-I and sphene-II are 2.33 and 3.43 μm , respectively. The surface area of sphene-I and sphene-II are very high ($>200\ \text{m}^2/\text{g}$) and become comparable with that of sphene-III (67 m^2/g) when calcined at 700°C.

TABLE 2
Particulate Properties of Sphene-I, Sphene-II, and Sphene-III Powders

Sphene	Powder density (g/cm ³)	50% average agglomerated particle size (μm)	Surface area (M ² /g)	Particle size (μm)
I	4.00	2.33	81	0.02
II	3.26	3.43	70	0.03
III	2.57	9.0	67	0.03

Sintering and Microstructure. The micrographs of sintered sphene-I, sphene-II, and sphene-III are shown in Figure 3. Sphene-I achieved 88% theoretical density when sintered at 1200°C for 2 h. The micrograph of the surface shows the presence of some open pores (Fig. 3a). When the sintering temperature was increased to 1300°C, the density became 96% of the theoretical value; a micrograph of the surface is shown in Figure 3b. The micrographs reveal the presence of densely packed grains in the sintered body; the grains are uniform in size ($\approx 1 \mu\text{m}$). The fine-grained microstructure of sintered sphene-I could be attributed to the mineralizing effect of fluoride ions.

Compacted sphene, derived from the sol-gel process (sphene-II), was sintered at 1200–1300°C for 2 h. Sphene-II achieved 85% theoretical density at 1200°C, and the density increased to 93% on sintering at 1300°C. The micrograph of the surface of a pellet sintered at 1200°C shows poor densification and the presence of pores (Fig. 3c). The micrograph shown in Figure 3d reveals the dense nature of the compact sintered at 1300°C. The grains are nearly diamond shaped with almost uniform grain size ranging from 2–4 μm . The smaller grain size and higher densification of sol-gel-derived sphene could be attributed to the lesser agglomeration in the powders. The scanning electron microscopy microstructure of sphene-III (1250°C) shows poor densification (83% theoretical density) and the presence of open pores with the grain sizes ranging from 2–4 μm . The fractograph of this specimen reveals the platelet nature of the particles, i.e., with irregular shapes (Fig. 3e). When the sintering temperature was increased to 1325°C, the bulk density increased to 92% theoretical value. The micrograph (Fig. 3f) of the surface reveals an almost pore-free state with large grains (5–10 μm). Sintering of sphene above 1325°C leads to melting that eventually reduces the sintered density.

CONCLUSIONS

Sphene (CaTiSiO_5) has been prepared by coprecipitation, sol-gel, and combustion processes. The crystallization and sintering of sphene is greatly influenced by the method of preparation. Single phase sphene formation occurs at a lower temperature (1000°C) in sphene-I compared with sphene-II and sphene-III ($\approx 1200^\circ\text{C}$). In sphene-II, small amounts of CaTiO_3 and cristobalite SiO_2 were seen as impurities even after calcination at 1200°C, due to the homocondensation of alkoxides. The coprecipitation-derived product (sphene-III) can be sintered to a high density (96% theoretical), and its micrograph will show a uniformly grained microstructure.

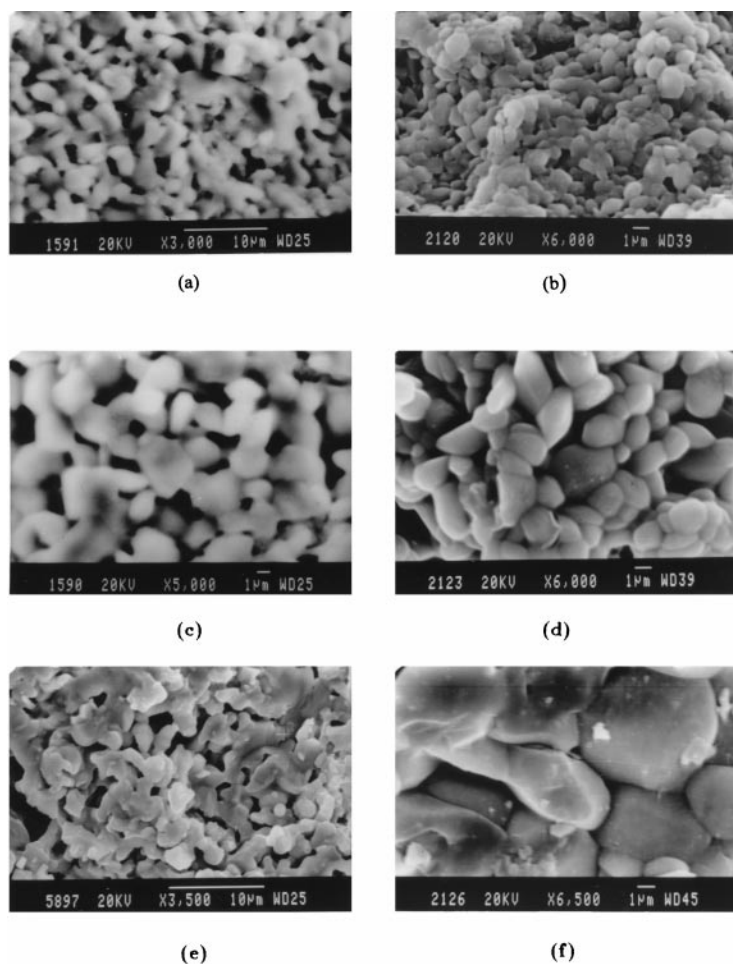


FIG. 3

Scanning electron micrographs: sphene-I at (a) 1200°C and (b) 1300°C; sphene-II at (c) 1200°C and (d) 1300°C; sphene-III at (e) 1250°C and (f) 1325°C.

REFERENCES

1. P.J. Hayward, in *Radioactive Waste Forms for the Future*, ed. W. Lutze and R.C. Ewing, p. 427, Elsevier, Amsterdam (1988).
2. E.R. Vance and D.K. Agrawal, *Nucl. Chem. Waste Mgt.* **3**, 229 (1982).
3. M. Muthuraman, N. Arul Dhas, and K.C. Patil, *Bull. Mater. Sci.* **17**, 977 (1994).
4. M. Muthuraman, K.C. Patil, S. Senbagaraman, and A.M. Umarji, *Mater. Res. Bull.* **31**, 1375 (1996).
5. M. Muthuraman and K.C. Patil, *J. Mater. Sci. Lett.*, In Press.
6. W. Lange, in *Fluorine Chemistry*, ed. J.H. Simons, p. 127, Academic Press, New York (1950).
7. B.E. Yoldas, *J. Mater. Sci.* **21**, 1087 (1986).
8. M. Jansen and E. Guenther, *Chem. Mater.* **7**, 2110 (1995).
9. S.K. Chen and H.S. Liu, *J. Mater. Sci.* **29**, 2921 (1994).
10. E.R. Vance, *Mater. Res. Bull.* **21**, 321 (1986).
11. P. Tartaj, C.J. Serna, and M. Ocana, *J. Am. Ceram. Soc.* **78**, 1147 (1995).